SGS analysis of the evolution equations of the mixture fraction and the progress variable variances in the presence of spray combustion

Hicham Meftah, Julien Reveillon, A. Mir, François-Xavier Demoulin

SGS analysis of the evolution equations of the mixture fraction and the progress variable variances in the presence of spray combustion

H. Meftah*, J. Reveillon*[1], A. Mir+, F.X. Demoulin*
(*) CORIA, INSA, Avenue de l'Université,
76800 Saint Etienne du Rouvray, France.
(+) ENSA, B.P.1136 Agadir, Maroc.

ABSTRACT

In this paper, direct numerical simulation databases have been generated to analyze the impact of the propagation of a spray flame on several subgrid scales (SGS) models dedicated to the closure of the transport equations of the subgrid fluctuations of the mixture fraction Z and the progress variable c. Computations have been carried out starting from a previous inert database [22] where a cold flame has been ignited in the center of the mixture when the droplet segregation and evaporation rate were at their highest levels. First, a RANS analysis has shown a brutal increase of the mixture fraction fluctuations due to the fuel consumption by the flame. Indeed, local vapour mass fraction reaches then a minimum value, far from the saturation level. It leads to a strong increase of the evaporation rate, which is also accompanied by a diminution of the oxidiser level. In a second part of this paper, a detailed evaluation of the subgrid models allowing to close the variance and the dissipation rates of the mixture fraction and the progress variable has been carried out. Models that have been selected for their efficiency in inert flows have shown a very good behaviour in the framework of reactive flows.

1 INTRODUCTION

Many industrial devices involve the turbulent combustion of an evaporating liquid phase. Numerous physical phenomena interact in combustion chambers. It begins with the atomization of liquid sheets at the injector outlet, followed by the dispersion of droplets generally embedded in a turbulent stream, to end with strongly coupled evaporation and combustion processes. One of the main challenge of turbulent combustion modelling is to account for the presence of the evaporating liquid phase in every stage of the physical process.

[1]Corresponding author: reveillon@coria.fr

A major input parameter of the non-premixed turbulent combustion models is the mixture fraction variable (denoted Z in this paper), which characterizes locally the mixing between the evaporated fuel and the gaseous oxidizer. Indeed, in Reynolds averaged formulations (RANS) or large eddy simulations (LES), the filtered or averaged mixture fraction Z, its variance Z_v and the corresponding dissipation rate χ_Z are necessary to estimate the local characteristic mixing delays and to generate presumed probability density functions [2] able to close the chemical source terms. It also allows for the localisation in flamelet libraries [18] or for the use of conditional moment closure methods [12].

Many works have been dedicated to the prediction of the mixture fraction evolution in purely gaseous flows where Z is an inert scalar: the evolution of its averaged value $\langle Z \rangle$ is classically established through an advection/diffusion equation although the determination of its variance $\langle Z_v \rangle$ and dissipation χ_Z is less straightforward; see for instance the works of [17, 16], and references therein. However, the difficulties are now well understood and many closures exist. But, when two phase flows are considered, the mixture fraction is no longer an inert scalar. Indeed, the appearance in the gas phase equations, of mass source terms due to the evaporation of the liquid phase modifies deeply the mixture fraction field. With respect to the local droplet density, Z fluctuations appear during the turbulent mixing and the local rise of mixture fraction gradients affects the dissipation rate. The formalism of these new source terms and their effects on the gas phase have been described in some recent studies: [21, 23, 6, 3] where new closures have been suggested. These models evaluate the new source terms appearing in the transport equations for mixture fraction mean and variance. They also take into account the evaporation effects on the dissipation rate and, thus, the mixing delay.

In a previous work [22], the authors have studied the links between the preferential segregation of the droplets and the mixture fraction evolution. Indeed, the presence of droplet clusters due to preferential segregation is important for global variables such as the mean vapour mass fraction $\langle Z \rangle$ and variance Z_v. Within a turbulent flow, three stages have been observed for droplet evaporation. First, there is no influence of clusters and an almost d-square law whose rate depends on isolated droplet characteristics is observed. Then, a cluster evaporation mode appears. Indeed, droplets are embedded in vapour pockets close to saturation. The evaporation rate of the droplets inside the cluster is strongly diminished, if not stopped. Finally, two evolutions are possible : either the lightest droplets are not able to leave the saturated area because of their lack of inertia.

Their evaporation rate is thus strongly related to the diffusion rate of the pocket of vapor toward the fresh gases. Either the turbulent motion contributes to dispersing the heaviest droplets, which may reach non-saturated areas to finish their evaporation process.

Mixture fraction variable is generally introduced when non-premixed combustion is implied. But in the case of spray combustion, the flow is mostly partially premixed. Then, it is necessary to introduce the progress variable c. It defines the reaction progress within the premixed mixture. In fresh gases, $c = 0$ whereas in burnt gases, $c = 1$. Note that the progress variable is not able to give any information about the initial equivalence ratio of the mixture. One of the difficulty of two-phase combustion modeling is that both Z and c may be necessary to feed turbulent combustion models if partially premixed combustion appears [24].

The objective of this paper is to use direct numerical simulation databases to analyze the impact of the propagation of a spray flame on several subgrid models dedicated to the closure of the balance equations of the subgrid fluctuations of Z and c. Computations are carried out starting from a previous inert database [22] and a cold flame is ignited in the mixture when the droplet segregation and evaporation rate are at their highest level.

A first RANS analysis allowing to observe the general impact of the propagation of the flame on the mixture fraction properties is carried out. It is followed by a detailed subgrid evaluation of the models allowing to close the variance and the dissipation rates of the mixture fraction and the progress variable.

In the subsequent sections, a brief description of the numerical procedures and the control parameters are detailed together with a description of the governing equations and the various hypotheses that have been used. Then, the evolution equations of the mixture fraction mean and variance as well as the progress variable equations are presented and the modeling of their various unclosed terms is discussed.

2 NUMERICAL PROCEDURE AND STATISTICS

The gaseous carrier phase is a forced isotropic homogeneous turbulence, which is resolved in a cubic domain with periodic boundary conditions. A discrete Lagrangian description allows for describing the vaporizing droplets. Various sets of governing equations are thus coupled together to carry out the computations. Because of the forcing procedure restrictions, the gas phase velocity is evaluated in spectral space. The evolution of the

fuel and oxidizer mass fractions is described in physical space so that it can be easily coupled with the Lagrangian description of the evaporating spray. The complete resolved equations may be found in [22], which was dedicated to inert flows. In the following, a brief summary of the configurations and the numerical procedure is presented. Then, an extension to reacting flows with constant density is used to study the impact of the fuel consumption on the turbulent mixing. This approach allows for an accurate forcing of the turbulence in the spectral space but a drawback, as far as combustion is concerned, is that flow dilation is ignored. Of course it is a major phenomena, but it is current to neglect it in basic studies to focus on some specific physical interaction effects. This work concentrate on the effect of temperature variation on cluster evaporation and on mixture fraction and progress variable evolution while a front flame propagates.

2.1 Numerical procedure

To maintain statistically stationary the main properties (energy, dissipation rate, integral scale) of the spectral turbulence, a controlled amount of energy must be transferred into the spectral simulation through a fully controlled deterministic forcing scheme [9] with an efficient convergence rate towards the model spectrum; this reduced drastically the fluctuations of the prescribed properties generally observed in other methods. Then, the following equation is resolved :

$$\frac{\partial \widehat{u}}{\partial t} = \widehat{a} + \frac{f_\kappa}{\tau_f}\,\widehat{u} \quad , \tag{1}$$

where $\widehat{a}$ represents the classical Navier-Stokes contributions. The forcing function f_κ is detailed in [9] and τ_f is a relaxation time smaller than the Kolmogorov time scale.

A one-way momentum coupling determines the droplet motion. However, to study the evolution of the mixture fraction released by the droplet evaporation, a two-way coupling is considered from the mass exchange point of view. The time evolution of species mass fractions is thus considered in a physical space to simplify their coupling with the dispersed phase:

$$\frac{\partial Y_\alpha}{\partial t} + \frac{\partial Y_\alpha u_i}{\partial x_i} = D_\alpha \frac{\partial^2 Y_\alpha}{\partial x_i^2} + \frac{1}{\rho}\dot{s}_\alpha \tag{2}$$

where D_α is the species diffusion coefficient and $\dot{s}_\alpha$ a mass source term due to the evaporation of the dispersed liquid phase. These equations are solved thanks to a third order Runge-Kutta procedure, which is already used for the spectral space. Similar sub time-steps are applied for both spectral and physical solvers. A sixth order Pade scheme [14]

is applied to determine the spatial derivatives.

A classical discrete Lagrangian approach is adopted to follow the monodispersed spray evolution within the gaseous oxidiser. By denoting $\mathbf{v}_k$ and $\mathbf{x}_k$ the velocity and position vectors of every droplet k, the following relations:

$$\frac{d\mathbf{v}_k}{dt} = \frac{1}{\beta_k^{(v)}}\left(\mathbf{u}\left(\mathbf{x}_k,t\right)-\mathbf{v}_k\right) \quad , \tag{3}$$

$$\frac{d\mathbf{x}_k}{dt} = \mathbf{v}_k \quad , \tag{4}$$

are used to track the evolutions of the droplets throughout the computational domain. The vector $\mathbf{u}$ represents the gas velocity at the droplet position $\mathbf{x}_k$. The right hand side term of equation 3 stands for a drag force applied to the droplet where $\beta_k^{(v)}$ is a kinetic relaxation time:

$$\beta_k^{(v)} = \frac{a_k^2}{a_0^2}\frac{\tau_p}{C_k} \quad . \tag{5}$$

a_k is the diameter of the droplet k and a_0 is the initial diameter of any droplet of the initially monodispersed spray. The characteristic kinetic time τ_p is defined by the relation

$$\tau_p = \frac{\rho_d a_0^2}{18\mu} \quad , \tag{6}$$

and a corrective coefficient C_k [5] is introduced to allow for the variation of the drag factor.

The characteristic evaporation time of the droplets is controlled by selecting an appropriate value for the saturation level Y^s [22]. The evaporation of every droplet in the flow accounts for the fuel mass fraction at the droplet surface Y_k^s and the local vapor level at the droplet position, $Y_F(\mathbf{x}_k)$. Saturation conditions mainly depend on the properties of the flow at the droplet's surface: temperature, pressure. In our simplified configuration, a constant saturation level such as $Y_k^s = Y^s$ is considered.

The following relation for the surface evolution of every "k" droplet may be written:

$$\frac{da_k^2}{dt} = -\frac{a_k^2}{\beta_k^{(a)}} \quad . \tag{7}$$

A classical model (d-square law) is to consider $\beta_k^{(a)} = cte$. It leads to a linear relation between droplet surface and time. However, in our simulation, saturation is accounted for and the characteristic relaxation time is defined by:

$$\beta_k^{(a)} = \frac{S_c}{4Sh_c}\frac{\rho_d}{\mu}\frac{a_k^2}{\ln\left(\frac{1-Y_F}{1-Y^s}\right)} \quad , \tag{8}$$

where $Sc = 0.7$ is the Schmidt number and Sh_c the convective Sherwood number, which is equal to 2 in a quiescent atmosphere; however, a correction must be applied in a convective environment. In this context, the empirical expression of Faeth and Fendell ([13]) has been used. The mean evaporation delay is controlled by selecting an appropriate value for the saturation level Y^s corresponding to the prescribed temperature level in the domain.

To account for masse exchange between both phases, droplet mass source terms have to be dispatched over the Eulerian nodes and the organisation of an accurate projection of those Lagrangian sources to the Eulerian mesh is still an open problem. In our simulations, each Lagrangian source is instantaneously distributed over the Eulerian nodes directly surrounding the droplet. This classic procedure leads to a grid dependence of the repartition. It induces a numerical dispersion that remains weak because of the small size of the DNS grid and the small turbulent Reynolds number [23], which leads to a weak slip velocity between the droplets and the carrier phase.

3 CONFIGURATION

The following four-stage procedure has been employed to analyse all the interactions between the turbulent flow and the dispersed phase [22] . Flame and dispersing particles have been plotted in Fig. 1 to illustrate the final configuration.

Stage 1: statistically stationary turbulence

In this preliminary stage, the turbulent gaseous phase evolves alone in a 129^3 Cartesian grid until its statistical properties reach a steady state thanks to the forcing procedure that keeps the mean kinetic energy $k = 3.375 m^2/s^2$ at the prescribed level. The maximum energy length l_0 is thus equal to $l_0 = L/7$ and remains constant. L is the cubical domain dimension equal to 3 mm. The velocity root mean square $u' = 1.5\ m/s$ is used as reference parameter along with the eddy turn-over time $\tau_0 = l_0/u'$ and the characteristic time of the velocity fluctuations τ_κ of the smallest structures ($\eta \approx 1.8\ 10^{-5} m$). The turbulent Reynolds number of the simulation is $Re_{l_0} = 43$.

Stage 2: spray dynamical equilibrium

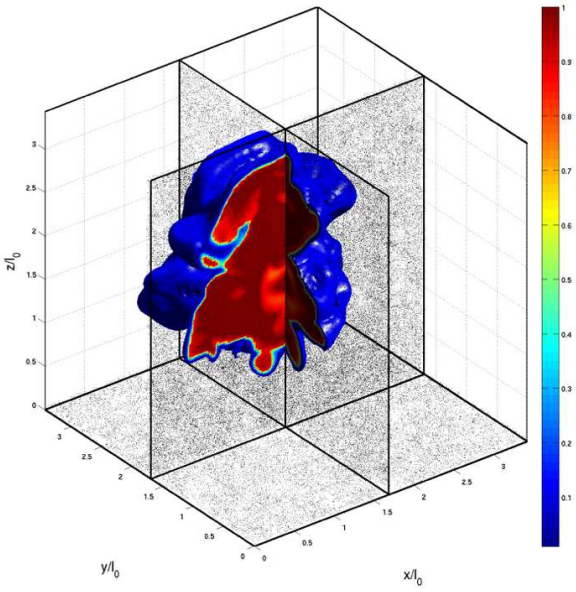

(a)

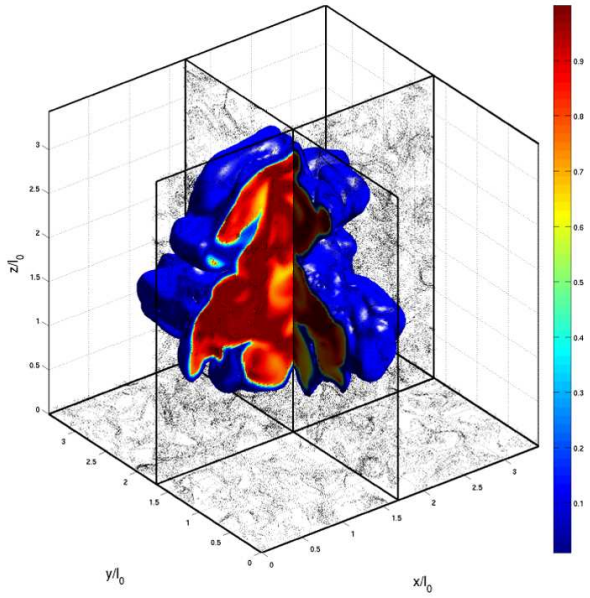

(b)

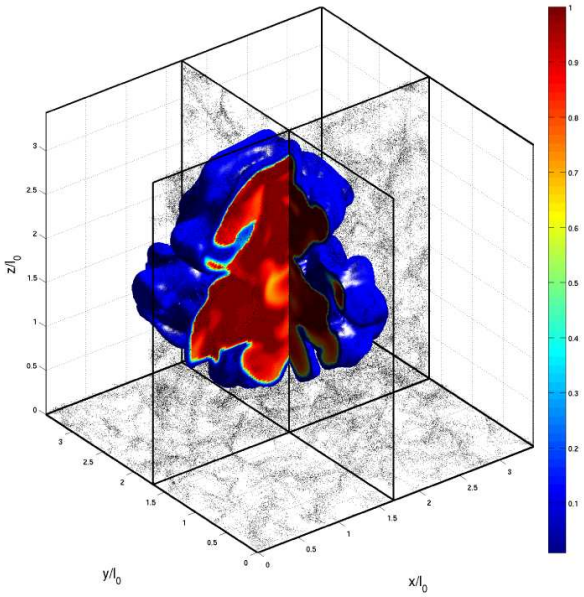

(c)

Figure 1: Spray concentration areas : black dots, (a): $St = 0.17$, (b): $St = 1.05$, (c): $St = 5.6$, isosurfaces : progress variable

Several eddy turn-over times after the turbulent flow reaches its stationary state, $N_d \approx$ 2150000 mono-dispersed non-evaporating particles are randomly embedded throughout the computational domain with a zero initial velocity. The drag force sets particles in motion. Then, the spray reaches a dynamical equilibrium with the turbulence. It corresponds to a stationary slip velocity standard deviation. Droplet dispersion is usually characterised by Stokes number $St = \tau_p/\tau_\kappa$ [26], which indicates the ability of droplets to capture local variations of the carrier phase velocity. Turbulence properties being fixed, simulations have been carried out by modifying the τ_p parameter. Three stokes numbers have been considered : 0.17, 1.05 and 5.6 corresponding to droplet diameters varying between 2 and 70 μm.

Stage 3: liquid phase evaporation and micro-mixing

Once the particles have reached a dynamical equilibrium with the surrounding turbulence, they are allowed to evaporate according to a specific characteristic evaporation delay τ_v prescribed by setting the saturation level in the surrounding atmosphere.

To describe the mixing between the gaseous fuel and the oxidiser, the usual definition of the mixture fraction Z is chosen [15, 20] leading to $Z = Y_F$ in an inert flow. A passive scalar is defined [15] as

$$\varphi = s_r Y_F - Y_O$$

where the stoichiometric mass ratio is $s_r = 11$ when considering the single step reaction $C_7H_{16} + 11O_2 \rightarrow 7CO_2 + 8H_2O$. Normalizing φ yields to the mixture fraction

$$Z = \frac{\Phi_o(Y_F/Y_{F,o}) - (Y_O/Y_{O,o}) + 1}{\Phi_o + 1} \tag{9}$$

with $Y_{F,o} = 1$, $Y_{O,o} = 0.23$ and $\Phi_o = s_r Y_{F,o}/Y_{O,o}$. Note that in the case of spray evaporation, Z cannot reach unity, but a local maximum level depending on saturation conditions. Consequently, a normalisation of Z is introduced by using the saturation limit Z_s. Z/Z_s is thus bounded between 0 and 1 and it is of practical interest for analysing correlations between the evaporating spray and the turbulent mixing.

Stage 4: flame ignition and propagation

To mimic the ignition of two-phase flow mixtures, a spherical kernel (diameter : 1 l_0) of burnt gases is generated at the centre of the domain. At the considered ignition time, gaseous fuel and oxidiser engulfed in this sphere are instantaneously transformed in burnt gases according to the chemical equilibrium defined by the above simple kinetic. Following a spray specific one-step Arrhenius law [25, 24] such as the maximum of the reacting rate corresponds to a stoichiometric mixture, the flame is then able to propagate. Because of the limitation of our numerical system, gas dilatation (due to the temperature elevation in burnt gases) has not been considered. Thus the propagating flame does not affect the carrier phase momentum. The Arrhenius law is activated with an artificial temperature field that is linearly estimated from the mass fraction of burnt gases (or products) Y_P :

$$T = T_u + Y_P(T_b - T_u) \tag{10}$$

The choice of the time of ignition is not arbitrary. It is made accordingly to the delay of evaporation of the spray. Indeed, there must be enough fuel in the domain to ignite the mixture but the evaporation process must be still active. Thus for an evaporation delay equal to $\tau_v = 0.25\tau_0$, the mixture has been ignited at $\tau_{ig} = 0.11\tau_0$, which corresponds to a maximum of the fluctuations of the mixture fraction level.

Premixed flame front propagation depends on the fresh gases temperature and equivalence ratio. The flame profile may be described thanks to the progress variable, which may be defined through mass fractions or temperature. We chose the temperature expression :

$$c = \frac{T - T_u}{T_b - T_u} \tag{11}$$

where T_u and T_b are the fresh gases and burnt gases temperature, respectively.

When necessary, the Reynolds averaging operator is applied following two procedures:

- $\langle A \rangle$ is the average of the field $A(x, y, z)$ over the three directions of the Cartesian grid.
$$\langle A \rangle = \frac{1}{L^3} \int_0^L \int_0^L \int_0^L A(x, y, z) dx dy dz$$
- When a spherical flame propagates, averaging may be carried out over a fixed radius:
$$\langle A \rangle_r = \frac{\int_0^{2\pi} \int_{-\pi}^{\pi} \int_r^{r+dr} A(r, \theta, \varphi) d\theta d\varphi dr}{\int_0^{2\pi} \int_{-\pi}^{\pi} \int_r^{r+dr} d\theta d\varphi dr}$$

	$St = 0.17$	$St = 1.05$	$St = 5.6$
$\tau_v = \infty$	A	B	C
$\tau_v = 1/2\tau_0$	A_1	B_1	C_1
$\tau_v = 1\tau_0$	A_2	B_2	C_2
$\tau_v = 2\tau_0$	A_3	B_3	C_3

Table 1: Configuration names, St : Stokes number, τ_v : evaporation delay. Non evaporating case : $\tau_v = \infty$

4 RANS ANALYSIS

Although homogeneous turbulence is a straightforward configuration, the addition of an evaporating dispersed phase allows us to be at the midpoint of many poorly understood interactions between turbulence, spray, mixing and combustion. To begin with, evaporation is considered in a classical RANS analysis. Once dynamical equilibrium is reached between the turbulent gaseous flow and the dispersed phase, evaporation is activated. Mixing between the fuel vapour and the gaseous oxidiser is characterised by the mixture fraction Z. Three cases have been chosen with three different initial Stokes numbers. They are recapitulated in table 1: cases B has a Stokes number close to unity when segregation is maximum, cases A and C correspond to low and high Stokes numbers, respectively. The liquid density fluctuations are the same but the characteristic cluster size and the droplet dynamics are very different. Various characteristic evaporation delays τ_v have been considered : (1) $\tau_v = 0.5\tau_0$, (2) $1\tau_0$, (3) $2\tau_0$. Configuration names are summarized in table 1. More analysis concerning inert flows may be found in [22].

The evolution of $\langle Z \rangle / Z_s$ is plotted in Fig. 2-(a) for cases A1, B1 and C1. It is clear from this figure that the most segregated case B1 takes the longest time to evaporate although a first order estimation (obtained thanks to the tangent of the curve at $t/\tau_0 = 0$) would give the same results for the three cases. Note that both configurations A1 and C1 start with exactly the same evolution of the mean mixture fraction. Indeed, the initial droplet dispersion level being the same in both cases, the evaporation rate is similar at first. No matter what the Stokes number of the droplets is, the mean mixture fraction evolution depends only on the initial segregation level of the particles. If the segregation level is small enough to avoid the creation of saturated pockets of fuel vapour, the evolution of $\langle Z \rangle$ may be easily estimated by a classical d-square law. On the other hand, if the segregation level and mass of liquid fuel are high enough for the pocket of vapour to reach

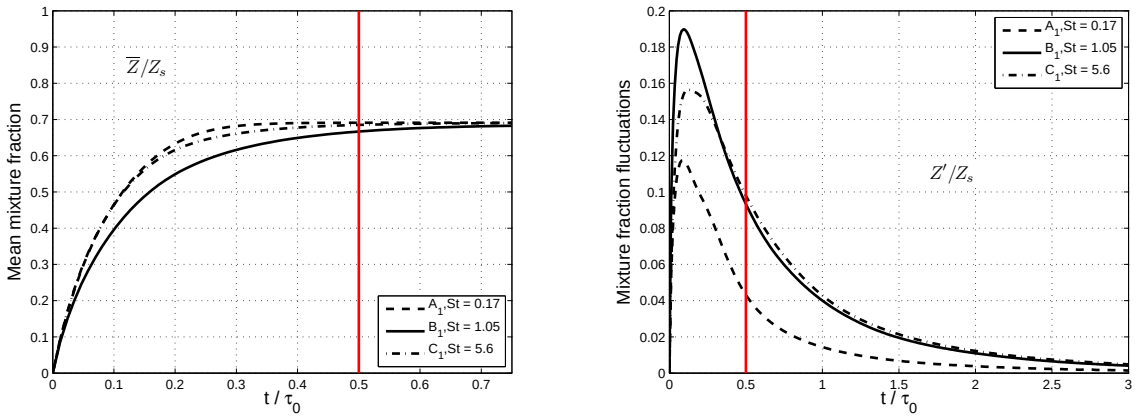

(a) (b)

Figure 2: Evolution of mixture fraction statistics in the domain, characteristic evaporation time : $0.5\tau_0$. Left : mean mixture fraction, right : deviation

the saturation limit, the evolution of $\langle Z \rangle$ is affected. Indeed, clusters containing a large number density of droplets are quickly surrounded by a high level of vapour concentration. Consequently, the gaseous fuel diffusion flux from the droplet surface to the surrounding gas is reduced because the saturation level is reached. It strongly decreases the evaporation rate for each droplet embedded in any cluster. Evaporation may even stop if the vapour concentration reaches locally the saturation limit. Consequently, the droplets need more time to evaporate. Some of them, generally the heaviest ones, do not follow the global motion of the cluster and reach areas where vapour concentration is low enough for them to evaporate. On the other hand, the smallest ones are in the cluster. In that case, the driving mechanism of the evaporation is linked to the global diffusive flux of vapour from the saturated cluster towards areas with low vapour concentration.

A different behaviour may be observed in Fig. 2-(b) where the evolution of the standard deviation of the mixture fraction : Z' has been plotted for cases A1, B1, C1. From a general point of view, the global shape of the curves is the same: starting from $Z'/Z_s = 0$ when evaporation starts, the curves reach a maximum value long before the characteristic evaporation delay (when $t/\tau_v \approx 0.2$). It is at this point that the dissipation of the mixture fraction fluctuations due to molecular diffusion becomes greater than the production due to the evaporation. Consequently, the mixture fraction fluctuations decrease continuously. Details of the competition between evaporation and dissipation may be found in [23].

Spray combustion involves three main phenomena : droplets dispersion, liquid evaporation and then combustion. This phenomena are coupled through strong interactions.

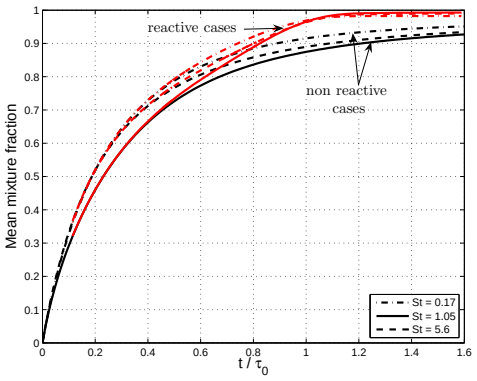

(a) - Mean mixture fraction $\langle Z \rangle / Z_s$

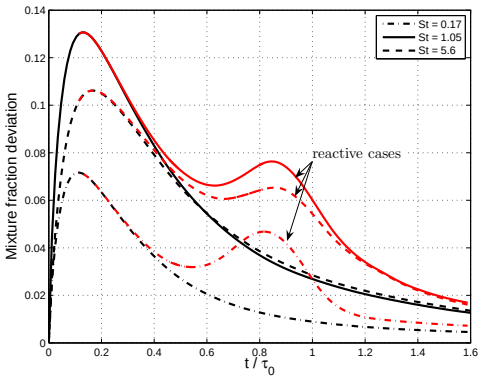

(b) - Mixture fraction deviation Z'/Z_s

Figure 3: Mixture fraction time evolution, inert cases (black lines) and reactive cases (red lines).

As we have seen previously, the topology of the mixture fraction field is srongly related to the Stokes number of the considered droplets. This dependance is still visible when combustion takes place and the flame structure and properties may be affected by the spray preferential segregation.

Evolution of $\langle Z \rangle / Z_s$ has been plotted in Fig. 3-(a) for the reference cases. Two configurations are plotted: with combustion and without combustion. As it was shown previously, the most segregated spray ($St = 1$) needs the longest time to be evaporated. Indeed, saturation prevents evaporation in the highly segregated areas. When combustion occurs, fuel pockets disappear and evaporation delay is reduced. Moreover the ends of the evaporation process takes place at the same time whatever the initial Stokes number. Hence, the dominant factor on evaporation is the combustion rather than the preferential segregation. At least in the cases studied in this work. The flame propagation has also an impact on the mixture fraction fluctuations Z'/Z_s whose evolution has been plotted in Fig. 3-(b). Indeed, a secondary peak appears on the curve, corresponding to a strong increase of the evaporation rate that may double the mixture fraction fluctuations. Because the combustion has a major effect on evaporation, it creates a mean gradient of the mixture fraction through the flame front. Thus the mixture fraction field is not homgeneous any more and an additional production term starts to play a role in the fluctuation of Z equation. This is the production by the mean scalar gradient that is well known in single phase flow. This term, combined with the production of fluctuation by evaporation, causes the second pic of mixture fluctuation.

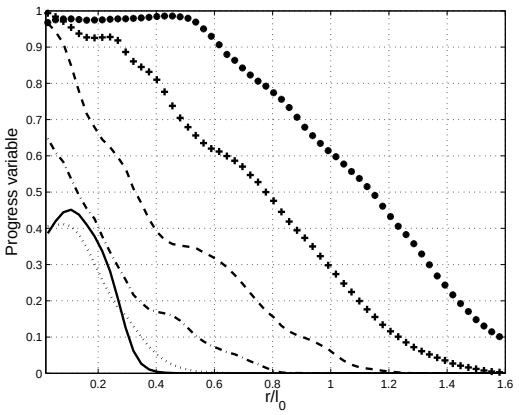

(a) - Mean progress variable for $\tau_v = 0.25\tau_0$

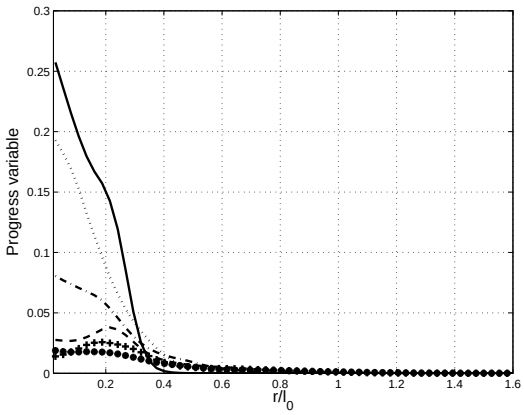

(b) - Mean progress variable for $\tau_v = \tau_0$

Figure 4: Progress variable evolution during the spherical flame propagation. From continuous line to symbol : positive time evolution.

An example of flame propagation issued from the DNS is shown in figure 1. Flame front propagation is strongly affected by the turbulent motion. The presence of the droplets modifies locally the mixture fraction and affect the flame shape as well. Figure 4-(a) shows the radial evolution of the progress variable which reaches a value of 1 only when all the droplets have been evaporated and the vapour of fuel is burnt. Combustion and evaporation are clearly interacting. Droplets affect flame propagation through their evaporation delay which control the flame. When evaporation is slow, compared to combustion delay, fuel vapour production is not enough and extinction occurs (figure 4-(b)).

5 *a priori* SGS ANALYSIS

To carry out an *a priori* analysis of the DNS fields, it is necessary to define a filtering operator. From a mathematical point of view, it is done thanks to a convolution between any turbulent signal Φ and a normalised filter function $G(x, \Delta)$, where Δ is the characteristic size of the filter function:

$$\overline{\Phi} = G \star \Phi = \int_{-\infty}^{+\infty} \Phi(x') G(x - x'; \Delta) dx' \tag{12}$$

In our work, a top hat filter has been applied :

$$G(x, \Delta) = \begin{cases} 1/\Delta & \text{if} \quad |x| \leq \Delta/2 \\ 0 & \text{otherwise} \end{cases} \tag{13}$$

with $\Delta = 5\delta x$ where δx is the DNS grid step. Generally, a Favre filtering process is defined in the framework of compressible flows :

$$\widetilde{\Phi} = \overline{\rho\Phi}/\overline{\rho} \tag{14}$$

In this paper, Favre filtered expression of the equations are presented to give the reader the complete compressible formulations of the equations and models. However, in this study, a constant density approach has been selected and $\widetilde{\Phi} = \overline{\Phi}$.

5.1 Subgrid variances

The mixture fraction subgrid variance is defined by :

$$\widetilde{Z_v} = \widetilde{Z^2} - \widetilde{Z}^2 \tag{15}$$

To obtain a clear picture of the phenomena controlling the subgrid variance, it is necessary to develop its balance equation. To begin with, the evolution equation of $\widetilde{Z^2}$ is written:

$$\begin{aligned} \frac{\partial\overline{\rho}\widetilde{Z^2}}{\partial t} + \nabla.(\overline{\rho}\widetilde{u}\widetilde{Z^2}) &= -\nabla.\overline{\tau}_{Z^2} + \nabla.(\overline{\rho}D\nabla\widetilde{Z^2}) - 2\overline{\rho}\widetilde{\chi}_Z \\ &\quad +2\overline{\rho}\widetilde{Z\dot{W}} - \overline{\rho}\widetilde{Z^2\dot{W}} \end{aligned} \tag{16}$$

where the dissipation $\widetilde{\chi}_Z$ is defined by:

$$\widetilde{\chi}_Z = \overline{\rho D|\nabla Z|^2}/\overline{\rho} \tag{17}$$

and,

$$\overline{\tau}_{Z^2} = (\overline{\rho u Z^2} - \overline{\rho}\widetilde{u}\widetilde{Z^2}) \tag{18}$$

Unclosed mass source terms due to the liquid phase evaporation appear in the second line of equation 16. From the modelling point of view, a possible way is to solve the evolution equation 16 of $\widetilde{Z^2}$ and then to define the mixture fraction variance by combining the result with equation 15.

On the other hand, it is possible to resolve directly:

$$\begin{aligned} \frac{\partial\overline{\rho}\widetilde{Z_v}}{\partial t} + \nabla.(\overline{\rho}\widetilde{u}\widetilde{Z_v}) &= -\nabla.\overline{\tau}_{Z_v} + \nabla.(\overline{\rho}D\nabla\widetilde{Z_v}) - 2\overline{\tau}_Z.\nabla\tilde{Z} - 2\overline{s}_{\chi Z} \\ &\quad +2\overline{\rho}(\widetilde{Z\dot{W}} - \widetilde{Z}\widetilde{\dot{W}}) - \overline{\rho}(\widetilde{Z^2\dot{W}} - \widetilde{Z}\widetilde{Z}\widetilde{\dot{W}}) \end{aligned} \tag{19}$$

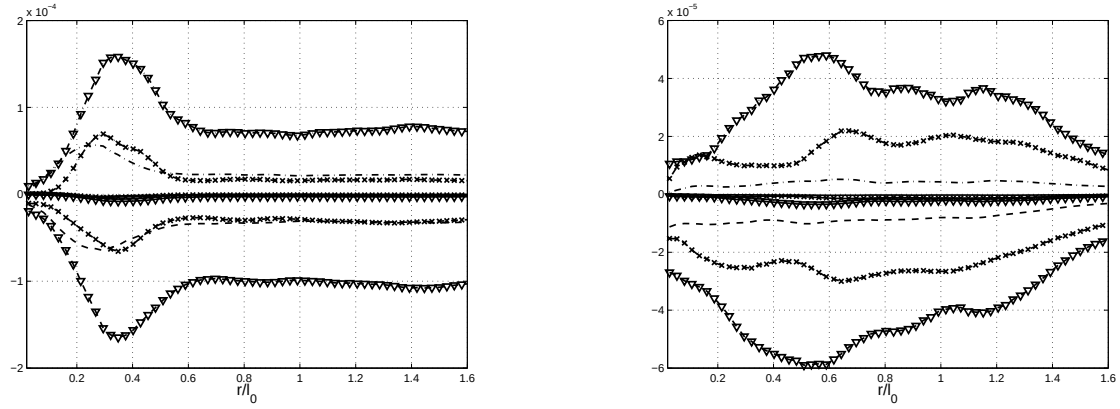

(a) - $t = 2\tau_{ig}$ (b) - $t = 6\tau_{ig}$

Figure 5: Radial contribution to the mixture fraction variance evolution $\langle -2\overline{s}_{\chi_Z}\rangle_r$: $--$; $\langle \overline{\rho}\widetilde{\dot{W}}^{+}\rangle_r$: $-\cdot-$; $\langle \overline{\rho}\widetilde{\dot{W}}^{-}\rangle_r$: line. without symbol : $St = 0.17$, (∇): $St = 1.05$, ($\times$): $St = 5.6$.

where

$$\overline{\tau}_{Z_v} = (\overline{\tau}_{Z^2} - 2\widetilde{Z}\overline{\tau}_Z)$$

$\overline{s}_{\chi_Z}$ is the sugrid part of the scalar dissipation rate. It is defined by

$$\overline{\rho}\widetilde{\chi}_Z = \overline{\rho D|\nabla Z|^2} = \overline{\rho}D|\nabla\widetilde{Z}|^2 + \overline{s}_{\chi_Z} \tag{20}$$

Again, the presence of evaporating droplets introduces two terms involving the evaporation rate:

$$\overline{\rho}\widetilde{\dot{W}}^{+} = 2\overline{\rho}(\widetilde{Z\dot{W}} - \widetilde{Z}\widetilde{\dot{W}}) \tag{21}$$

$$\overline{\rho}\widetilde{\dot{W}}^{-} = -\overline{\rho}(\widetilde{Z^2\dot{W}} - \widetilde{Z}\widetilde{Z}\widetilde{\dot{W}}) \tag{22}$$

To evaluate the order of magnitude of these terms in the subgrid variance equation, they have been plotted in figure 5 and compared to the dissipation term. It appears that $\overline{\rho}\widetilde{\dot{W}}^{-}$ is several order of magnitude smaller than both $\overline{\rho}\widetilde{\dot{W}}^{+}$ and the subgrid mixture fraction dissipation $2\overline{s}_{\chi_Z}$. Note that, $\overline{\rho}\widetilde{\dot{W}}^{+}$ is of the same order of magnitude than the dissipation. Similar conclusions have already been showed in the framework of inert simulations carried out in Pera *al* [1] and Reveillon and Vervisch [23]. In this study, one has to keep in mind that a turbulent spherical flame, fed by the vapour of fuel, is propagating along the radius.

A first conclusion may be drawn. As for the inert case, a closure of the subgrid variance $\widetilde{Z_v}$ equation is mainly based on a successful modelling of both $\widetilde{\dot{W}}^{+}$ and $\overline{s}_{\chi_Z}$, which strongly depend on the Stokes number as it may be observed in figure 5. A unitary Stokes number,

which leads to a highly segregated flow, has the strongest impact on the mass source terms but also on the dissipation term. The smallest droplets ($St = 0.17$) have a weak effect and the heaviest ones ($St = 5.6$) offers intermediary results. Indeed, at first, droplets are dispersed because of the ballistic trajectories before they reach a unitary Stokes number during their evaporation.

Similarly to the mixture fraction, the mixture fraction variance may be defined by:

$$\widetilde{c_v} = \widetilde{cc} - \widetilde{c}\widetilde{c} \tag{23}$$

From the evolution equation of the progress variable c:

$$\frac{\partial \rho c}{\partial t} + \nabla.(\rho u c) = \nabla.(\rho D \nabla c) + \rho \dot{\omega}_c \tag{24}$$

where $\dot{\omega}_c$ is the chemical source term, it is possible to develop an evolution equation for the subgrid variance of the progress variable:

$$\begin{aligned} \frac{\partial \overline{\rho}\widetilde{c_v}}{\partial t} + \nabla.(\overline{\rho}\widetilde{u}\widetilde{c_v}) &= -\nabla.\overline{\tau}_{c_v} + \nabla.(\overline{\rho}D\nabla\widetilde{c_v}) - 2\overline{\tau}_c.\nabla\tilde{c} - 2\overline{s}_{\chi_c} \\ &\quad + 2\overline{\rho}(\widetilde{c\dot{\omega}_c} - \widetilde{c}\widetilde{\dot{\omega}_c}) - \overline{\rho}(\widetilde{c^2\dot{W}} - \widetilde{cc}\widetilde{\dot{W}}) \end{aligned} \tag{25}$$

As for the subgrid variance $\widetilde{Z_v}$ equation, a new source term due to the droplet evaporation appears in the equation. Another one is directly linked to the chemical sources terms.

$$\overline{\rho}\widetilde{\dot{\omega}_c}^{+} = 2\overline{\rho}(\widetilde{c\dot{\omega}_c} - \widetilde{c}\widetilde{\dot{\omega}_c}) \quad \textit{chemical term} \tag{26}$$

$$\overline{\rho}\widetilde{\dot{\omega}_v}^{-} = -\overline{\rho}(\widetilde{c^2\dot{W}} - \widetilde{cc}\widetilde{\dot{W}}) \quad \textit{evaporation term} \tag{27}$$

In figure 6 the radial evolution of the chemical source term $\overline{\rho}\widetilde{\dot{\omega}_c}^{+}$ has been plotted along with the one due to the droplets evaporation $\widetilde{\dot{\omega}_v}^{-}$ and the corresponding subgrid dissipation term $\overline{s}_{\chi_c}$. It appears that the impact of the evaporation source term on the evolution of the variance of the progress variable is minimal. Indeed, prevalent terms are the chemical subgrid correlations $\widetilde{\dot{\omega}}^{+}$ and the dissipation $\overline{s}_{\chi_c}$. From the mixture fraction point of view, the scalar dissipation balances the vaporisation source terms. However, as far as the progress variable is concerned, an equilibrium takes place between the chemical source term and the scalar dissipation whereas vaporisation impact is weak. These terms need closures in order to estimate the progress variable variance evolution during an effective LES computation. An important point is the fact that the Stokes number of the droplets and therefore the preferential segregation of the droplets has no noticeable effect on the subgrid terms of the progress variable contrary to the mixture fraction.

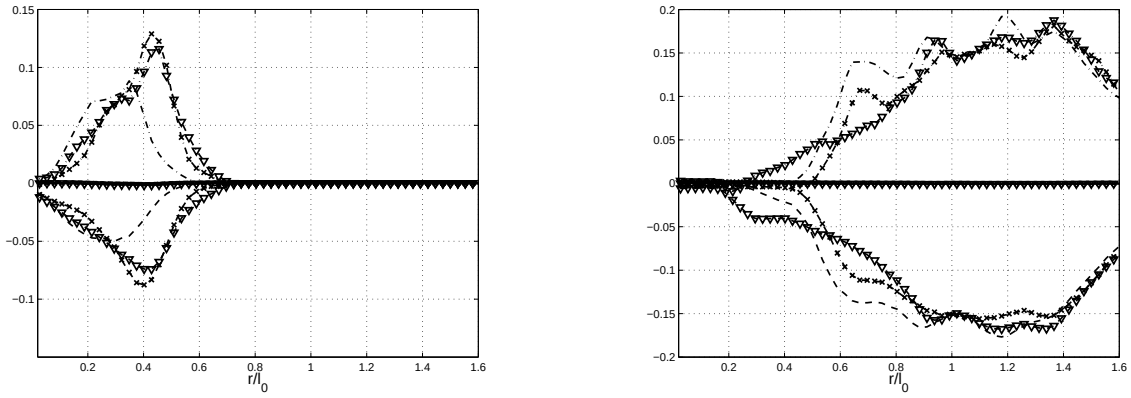

(a) - $t = 2\tau_{ig}$ (b) - $t = 6\tau_{ig}$

Figure 6: Radial contribution to the progress variable variance evolution $\langle -2\overline{s}_{\chi_c} \rangle_r$: $--$; $\langle \overline{\rho}\widetilde{\dot{\omega}}^{+} \rangle_r$: $-\cdot-$; $\langle \overline{\rho}\widetilde{\dot{\omega}}^{-} \rangle_r$: line. without symbol : $St = 0.17$, ($\triangledown$): $St = 1.05$, ($\times$): $St = 5.6$.

5.2 Subgrid variances modelling

One of the first models that has been developed to close the mixture fraction subgrid variance in the framework of gaseous combustion has been developed by Cook and Riley [4]. They used a scale similarity assumption to develop a simple expression for $\widetilde{Z_v}$:

$$\widetilde{Z_v} = \widetilde{ZZ} - \widetilde{Z}\widetilde{Z} = C_v^s \big[\widehat{\widetilde{Z}\widetilde{Z}} - \widehat{\widetilde{Z}}\widehat{\widetilde{Z}} \big] \tag{28}$$

where C_v^s is an unknown coefficient to be determined.

This model has been successfully employed in purely gaseous flows, even if the determination of the coefficient remains a stumbling block. However, it seems difficult to apply this model as far as two-phase flows are concerned. Indeed, C_v^s is generally considered as a constant. If this hypothesis may be applied in gaseous flows because of some direct correlations between large and small scales fluctuations, it is not the case if evaporating droplets are present. Local preferential segregation of evaporating droplets leads to peaks of small scales fluctuations that may not appear at the large scale level. This hypothesis has been confirmed by the work of Pera et al [1]. Knowing that no satisfactory dynamical procedure has been found, it is suggested to resolve the subgrid variance transport equation. A few years later, Domingo et al [8] have tested a scale similarity model to mimic progress variable variance $\widetilde{c_v}$ in the framework of a turbulent V flame. They showed also that the presence of a chemical source term has a prevalent effect on the progress variable field. Results were not encouraging and the $\widetilde{c_v}$ field was not properly captured. A

possible alternative, proposed by Pierce et Moin [19] for a purely gaseous flow is to use the following model:

$$\widetilde{Z_v} = C_Z \Delta^2 |\nabla \widetilde{Z}|^2 \tag{29}$$

where C_Z is a dynamical coefficient classically determined thanks to a test filter. If an evaporating liquid phase is present, it is possible to write

$$\widetilde{Z_v} = C_{zs} \left(C_Z \Delta^2 |\nabla \widetilde{Z}|^2 + \frac{\bar{\rho} \widetilde{\dot{W}^+}}{C_s^2 |\widetilde{S}|} \right) \tag{30}$$

with C_s, the Smagorinsky coefficient and C_{zs} a new dynamical coefficient. But, in the framework of DNS analysis, this model does not give satisfactory results neither for the mixture fraction variance [1] nor for the progress variable variance [8].

These difficulties are mainly due to the model concept. Indeed, these models are strictly based on the local properties of the turbulence but they do not really take into account the presence of the evaporating liquid phase.

Therefore, the resolution of a transport equation for the mixture fraction variance and the progress variable variance seems to be the more promising solution although it is the more complex. To do so, standard terms issued from the gas phase evolution may be closed with models developed in the framework of purely gaseous combustion. However, four main terms need specific closure as far as two-phase flows are concerned:

- the mass source term $\widetilde{\dot{W}^+}$,
- the dissipation $\overline{s}_{\chi_Z}$ of the mixture fraction variance equation,
- the chemical source term $\widetilde{\dot{\omega}^+}$,
- the dissipation $\overline{s}_{\chi_c}$ of the progress variable variance equation.

5.2.1 Subgrid source terms modelling

Modelling the prevalent source terms in both equations of the mixture fraction and progress variable variances consist into mimicking correlations between the mixture fraction and the evaporation rate $\widetilde{Z\dot{W}}$ and the progress variable and the chemical source term $\widetilde{c\dot{\omega}_c}$. As it has been exposed since the beginning of this paper, three phenomena are strongly coupled : spray dispersion (and preferential segregation) , droplet evaporation and chemical reactions. Our objective is to be able to characterise the prevalent correlations.

Following a RANS formulation of Hollmann et Gutheil [10], Pera et al [1] suggested a new model to estimate the mass source term $\widetilde{Z\dot{W}}$. The principle of the model is to separate $\widetilde{Z\dot{W}}$ into a correlated and an uncorrelated term:

$$\widetilde{Z\dot{W}} = \alpha\widetilde{\dot{W}}\frac{\widetilde{Z^2}}{\widetilde{Z}} + (1-\alpha)(\widetilde{Z}\widetilde{\dot{W}}) \tag{31}$$

where α is a correlation coefficient. In this work, we suggest to write a similar expression for the chemical source term of the progress variable equation:

$$\widetilde{c\dot{\omega}_c} = \alpha_c\widetilde{\dot{\omega}}_c\frac{\widetilde{c^2}}{\widetilde{c}} + (1-\alpha_c)(\widetilde{c}\widetilde{\dot{\omega}}_c) \tag{32}$$

Therefore for both variance equations, we have :

$$\widetilde{\dot{W}}^{+} = 2(\widetilde{Z\dot{W}} - \widetilde{Z}\widetilde{\dot{W}}) = 2\alpha_Z\widetilde{Z}_v(\frac{\widetilde{\dot{W}}}{\widetilde{Z}}) \tag{33}$$

and

$$\widetilde{\dot{\omega}}^{+} = 2(\widetilde{c\dot{\omega}_c} - \widetilde{c}\widetilde{\dot{\omega}_c}) = 2\alpha_c\widetilde{c}_v(\frac{\widetilde{\dot{\omega}}}{\widetilde{c}}) \tag{34}$$

Comparisons between the exact correlation terms and its corresponding model are presented in Fig. 7 and Fig. 8. In fact, when $\alpha_c = 1$, closure of the chemical source term (Eq. 8) in the progress variable variance equation offer a very good agreement and results very close to the one offered by the DNS have been found. A similar conclusion may be drawn concerning the mixture fraction variance closure.

5.2.2 Dissipation closures

The dissipation term is as important as the various source terms in the variance equations. Of course, there exist classical closures developed in the framework of gaseous combustion. However, as soon as an evaporating spray is present in the gas phase, the local gradients of vapour of fuel generally increases and the dissipation is the results of two counteracting phenomena : droplets evaporation and the usual gaseous diffusion. Thus, to close properly the dissipation term, the presence of the liquid phase has to be accounted for. Among the various possible approaches, we chose to evaluate the linear relaxation model and the equilibrium model.

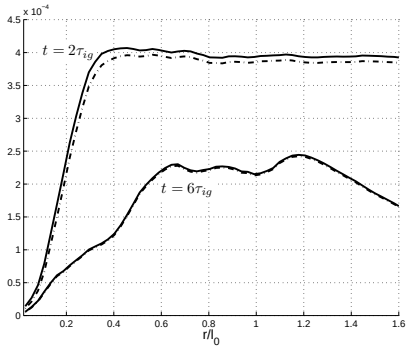

(a) - $St = 0.17$

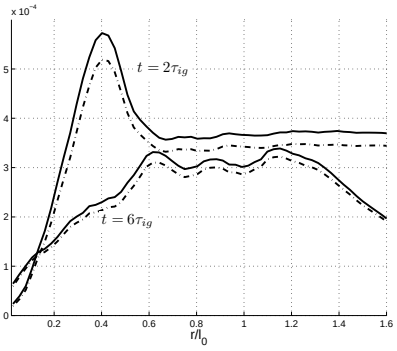

(b) - $St = 1.05$

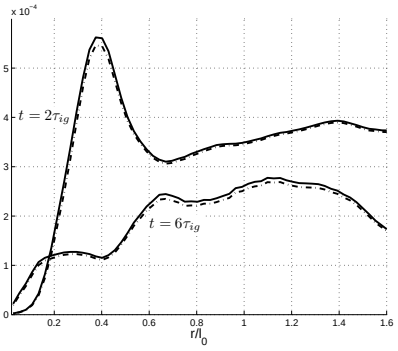

(c) - $St = 5.6$

Figure 7: Mixture fraction mass source term : model ($\widetilde{\langle Z\dot{W}\rangle}_r$, eq.33, dashed lines) comparisons with exact data from DNS (continuous line).

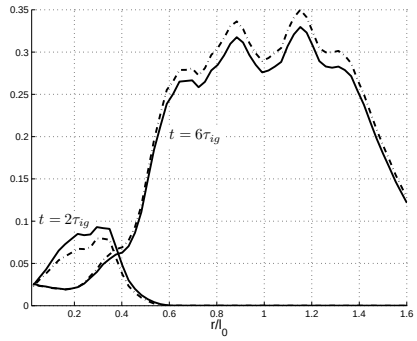

(a) - $St = 0.17$

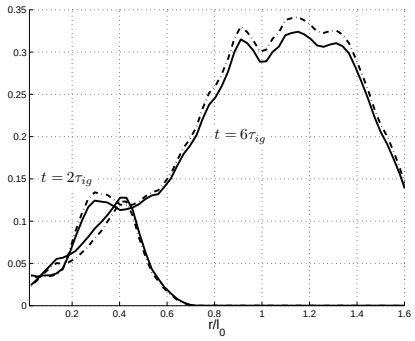

(b) - $St = 1.05$

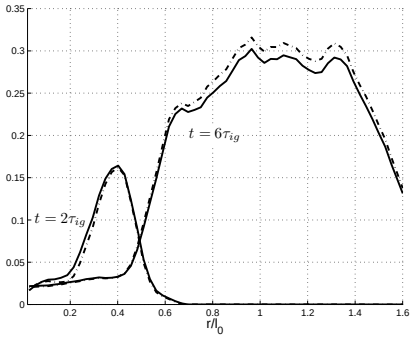

(c) - $St = 5.6$

Figure 8: Progress variable chemical source term : model ($\langle \widetilde{c\dot{\omega}_c} \rangle_r$, eq.34, dashed lines) comparisons with exact data from DNS (continuous line).

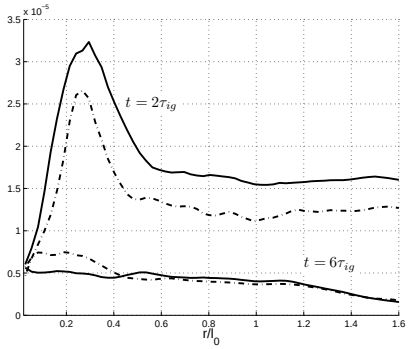

(a) - $St = 0.17$

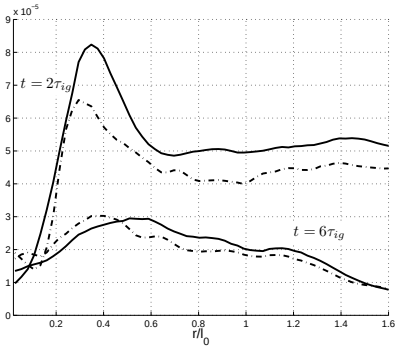

(b) - $St = 1.05$

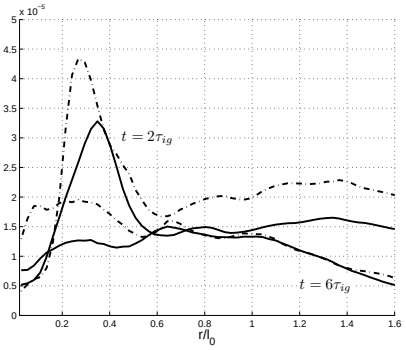

(c) - $St = 5.6$

Figure 9: Mixture fraction dissipation : relaxation model ($\langle \overline{s}_{\chi_Z} \rangle_r$, eq.43, dashed lines) comparisons with exact data from DNS (continuous line).

5.2.3 Linear relaxation model

The linear relaxation hypothesis is very usual in the framework of RANS simulations. It allows to estimate the dissipation rate from the local mixing characteristic delay. An adaptation of this model to the LES formulation gives:

$$\overline{s}_{\chi Z} = \bar{\rho}\frac{\widetilde{Z_v}}{\widetilde{\tau_Z}} \tag{35}$$

This equation is a straightforward description of the micro-mixing thanks to a characteristic mixing time $\widetilde{\tau_Z}$, which is supposed to be proportional to the turbulent characteristic time. Jimenez et al [11] suggested to consider that $\widetilde{\tau_Z}$ is proportional to the subgrid kinetic energy $\widetilde{k}$ and its corresponding dissipation rate $\widetilde{\epsilon}$. They used a Smagorinsky formulation:

$$\widetilde{\epsilon} = 2(\nu + C_s^2\widetilde{\Delta}^2|\widetilde{S}|)\widetilde{S}\widetilde{S} \tag{36}$$

and the Yoshizawa expression for the subgrid kinetic energy:

$$\widetilde{k} = 2C_I\widetilde{\Delta}^2\widetilde{S}\widetilde{S} \tag{37}$$

Eventually, they obtained:

$$2\widetilde{\chi}_Z = \frac{(\nu + C_s^2\Delta^2|\widetilde{S}|)}{S_c C_I \Delta^2}\widetilde{Z_v} \tag{38}$$

where C_I and C_S are constant to be determined. In a similar approach, Pera et al[1] suggested to write:

$$\overline{s}_{\chi Z} = C_\chi^*\frac{\overline{\rho}\widetilde{Z_v}}{(\Delta^2/\nu_t)} \tag{39}$$

and then, they used the Smagorinsky expression for the turbulent viscosity:

$$\nu_t = (C_s\Delta)^2|\widetilde{S}| \tag{40}$$

where $|\widetilde{S}| = (2\widetilde{S}\cdot\widetilde{S})^{1/2}$ is the contraction of the stress tensor

$$\widetilde{S} = \frac{1}{2}(\nabla\widetilde{u} + \nabla^T\widetilde{u}) \tag{41}$$

and, eventually

$$\overline{s}_{\chi Z} = C_\chi|\widetilde{S}|\overline{\rho}\widetilde{Z_v} \tag{42}$$

Very recently, Domingo et al [7] used a similar approach to determine the scalar dissipation rate in a gaseous configuration. They applied it for both the mixture fraction and the

progress variable. In this part, we propose to test them in our two-phase configuration. Formulations of the models are:

$$\overline{s}_{\chi Z} = C_{\chi Z}|\widetilde{S}|\overline{\rho}\widetilde{Z_v} \tag{43}$$

and

$$\overline{s}_{\chi_c} = C_{\chi_c}|\widetilde{S}|\overline{\rho}\widetilde{c_v} \tag{44}$$

where $C_{\chi Z}$ and C_{χ_c} are two constants to be determined.

In Fig. 9 and 10, it is possible to see the comparison between these models and the DNS results. When $C_{\chi_c} = 1$, the closure of Eq 44 is quite accurate. The global shape of the subgrid dissipation rate of the progress variable is well captured. Similar good results where observed in purely gaseous flows, with the same value of the constant by Domingo et al [7].

On the other hand, the closure of Eq. 43 allowing to estimate $\overline{s}_{\chi Z}$ has been carried out with the following constant value: $C_{\chi Z} = 0.6$. As it is shown in Fig. 9, the global shape of the dissipation rate of the mixture fraction variance is not well captured for all Stokes numbers. It means that the local segregation of the droplets affect the model results. Even if the global value is well captured, a dynamical estimation of the constant would improve the procedure.

5.2.4 Equilibrium model

In the framework of a purely gaseous flow, Pierce et Moin [19] used an equilibrium hypothesis between production and dissipation terms to estimate the subgrid variances thanks to the resolved fields. In 2006, Pera et al [1] used this model with inert two-phase flows estimate the mixture fraction subgrid dissipation. By using a gradient type closure, they wrote :

$$\overline{s}_{\chi Z} = -\overline{\tau}_Z \cdot \nabla\widetilde{Z} + \frac{\widetilde{\overline{\rho}\dot{W}^+}}{2} = \overline{\rho}(\nu_t/S_{ct})|\nabla\widetilde{Z}|^2 + \frac{\widetilde{\overline{\rho}\dot{W}^+}}{2} \tag{45}$$

with $D_t = \nu_t/S_{ct}$ the turbulent diffusion term, which may be written

$$D_t = C_Z\Delta^2|\widetilde{S}| \tag{46}$$

Eventually, the model expression is

$$\overline{s}_{\chi Z} = C_Z\overline{\rho}\Delta^2|\widetilde{S}|\nabla\widetilde{Z}|^2 + \frac{\widetilde{\overline{\rho}\dot{W}^+}}{2} \tag{47}$$

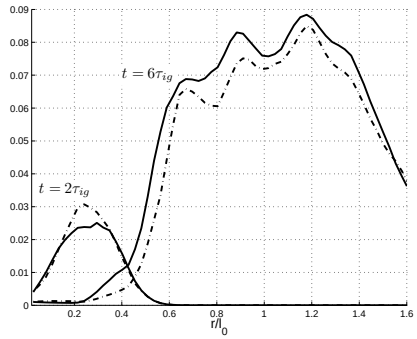

(a) - $St = 0.17$

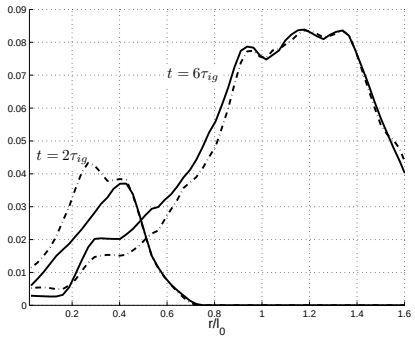

(b) - $St = 1.05$

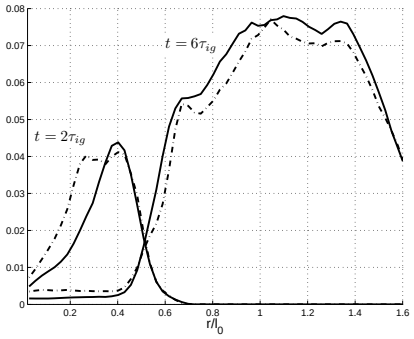

(c) - $St = 5.6$

Figure 10: Progress variable dissipation : relaxation model ($\langle \overline{s}_{\chi_c} \rangle_r$, eq.44, dashed lines) comparisons with exact data from DNS (continuous line).

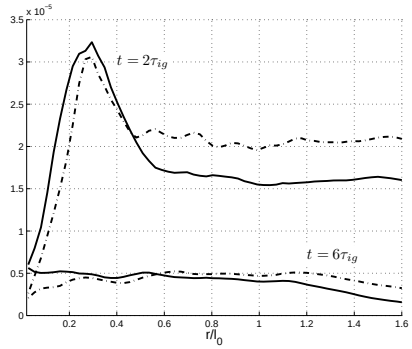

(a) - $St = 0.17$

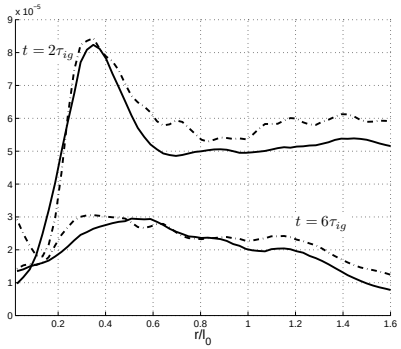

(b) - $St = 1.05$

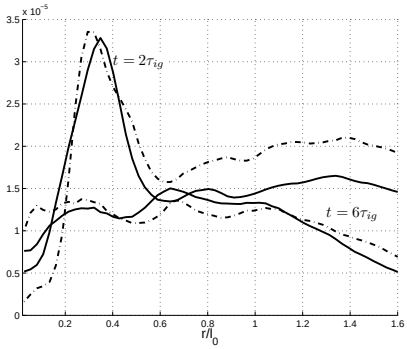

(c) - $St = 5.6$

Figure 11: Mixture fraction dissipation : equilibrium model ($\langle \overline{s}_{\chi_Z} \rangle_r$, eq.47, dashed lines) comparisons with exact data from DNS (continuous line).

With C_Z, a constant to be determined. In this work, we propose to use a similar formulation for the estimation of the subgrid dissipation rate of the progress variable.

$$\overline{s}_{\chi_c} = C_c \overline{\rho} \Delta^2 |\widetilde{S}| \nabla \widetilde{c}|^2 + \frac{\overline{\rho} \widetilde{\dot{\omega}}^+}{2} \tag{48}$$

Comparisons between DNS and the closure of Eq. 47 and 48 are presented in figure 11 and 12. When $C_Z = 0.08$ and $C_c = 0.12$, it appears that a good agreement may be observed. The global shape of the dissipation rate of the progress variable is captured. However, results are less satisfactory as far as the mixture fraction dissipation $\overline{s}_{\chi_Z}$ is concerned. The error on the mixture fraction dissipation when compared to the DNS is identical to the one obtained with the algebraic closure (Fig. 9) in the fresh gases : about 15 %. Outside of this zone, in the flame front and in the burnt gases, the equilibrium model compare well with the DNS. Again, a Stokes number dependance of the model constants could improve the results.

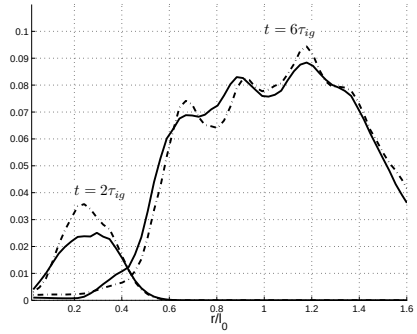

(a) - $St = 0.17$

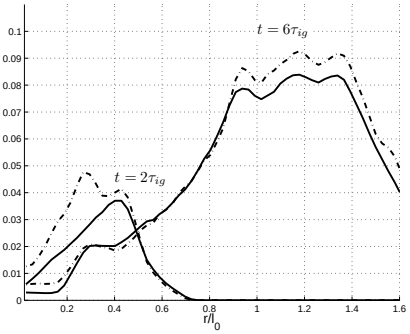

(b) - $St = 1.05$

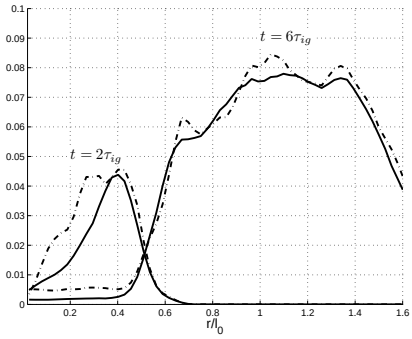

(c) - $St = 5.6$

Figure 12: Progress variable dissipation : equilibrium model ($\langle \overline{s}_{\chi_c} \rangle_r$, eq.48, dashed lines) comparisons with exact data from DNS (continuous line).

6 CONCLUSION

Statistically stationary turbulence is used as carrier phase to study spray dispersion, evaporation and combustion thanks to a spectral DNS solver that allows a physical forcing of the turbulence. The evolution of the dispersed liquid phase is modelled using a Lagrangian description. A one-way coupling is applied between the Eulerian and Lagrangian solvers as far as the momentum field is concerned. However, for the description of the vapour mass fraction evolution a two-way coupling has been used. Consequently, turbulent flow characteristics remain constant while the dispersion of various sprays is studied. The sole effect of the droplet dynamics has thus been isolated and characterised for various sprays by prescribing various Stokes numbers.

If the dispersion of non-evaporating droplets is first considered. It shows the formation of clusters of particles whose size and dynamics are strongly dependent on the considered Stokes number. When droplet evaporation occurs, the consequences of preferential segregation on the whole evaporation process lead to various mixture fraction fields. Flame ignition is done thanks to a premixed kernel in the centre of the computational domain.

A joint analysis of the mixture fraction and the progress variable has been carried out. Following the positive conclusions of former works dedicated to non-reactive two-phase flows or reactive one-phase flow, we decided to focus on the evolution equations of the subgrid mixture variances of the mixture fraction and the progress variable. Models dedicated to the estimation of the production of fluctuations due to evaporation and chemical reactions have been suggested and tested. These models have a very good behaviour when compared to the exact value extracted from DNS. Both reactive and non reactive scalar dissipation models are adressed in the context of LES formulation. Algebric or equilibrium closures give accurate result as far as the scalar dissipation in reactive flows is concerned. But the scalar dissipation in inert flows is more sensitive to the evaporation process. The algebric closure allows only the mean feature of the scalar dissipation to be recovered. Equilibrium hypothesis leads to a new model that incorporates directly the effect of evaporation. Some improvments are obtained with this model when compared to DNS data.

To conclude, two interesting points may be underlined. First, the mixture fraction evolution depends strongly on the Stokes number of the dispersing droplets. It affects the result of the various models that use generally constant coefficients or dynamic co-

efficients that do not depend on the local properties of the spray. However, the error remains reasonable. On the other hand, because chemical effects are prevalent compared to evaporation effects, the subgrid variance of the progress variable is not affected by the droplets dynamics.

7 ACKNOWLEDGEMENTS

This work received funding from the European Community through the project TIMECOP-AE (Project AST5-CT-2006-030828). It reflects only the author's views and the Community is not liable for any use that may be made of the information contained therein.

References

[1] C. Pera ans J. Reveillon, L. Vervisch, and P. Domingo, *Modeling subgrid scale mixture fraction variance in les of evaporating spray.*, Combustion and Flame (2006), no. 146, 635–648.

[2] R. Borghi, *Turbulent combustion modelling*, Prog. Energy Combust. Sci. **14** (1988), 245–292.

[3] O. Colin and A. Benkenida, *A new scalar fluctuation model to predict mixing in evaporating two-phase flows*, Combustion and Flame **134** (2003), 207–227.

[4] A. W. Cook and J. J. Riley, *A subgrid model for equilibrium chemistry in turbulent flows*, Phys. Fluids **6** (1994), no. 8, 2868–2870.

[5] C. Crowe, M. Sommerfeld, and Y. Tsuji (eds.), *Multiphase flows with droplets and particles*, CRC Press, 1998.

[6] F.X. Demoulin and R. Borghi, *Modeling of turbulent spray combustion with application to diesel like experiment*, Combustion and Flame **129** (2002), 281–293.

[7] P. Domingo, L. Vervisch, and D. Veynante, *Large-eddy simulation of a lifted methane jet flame in a vitiated coflow.*, Combustion and Flame (2008), no. 152, 415–432.

[8] Pascale Domingo, Luc Vervisch, Sandra Payet, and Raphael Hauguel, *Dns of a premixed turbulent v flame and les of a ducted flame using a fsd-pdf subgrid scale slosure with fpi-tabulated chemistry.*, Combustion and Flame (2005), no. 143, 566–586.

[9] L. Guichard, J. Reveillon, and R. Hauguel, *Direct numerical simulation of statistically stationary one- and two-phase turbulent combustion: a turbulent injection procedure*, Flow, turbulence and combustion **73** (2004), 133–167.

[10] C. Hollmann and E. Gutheil, *Modeling of turbulent spray diffusion flames including detailed chemistry*, Twenty-Sixth Symposium (International) on Combustion/The Combustion Institute, 1996, pp. 1731–1738.

[11] C. Jiménez, F. Ducros, B. Cueno, and B. Bédat, *Subgrid scale variance and dissipation of a scalar field in large eddy simulations*, Phys. Fluids **13** (2001), no. 6, 1748–1754.

[12] A.Y. Klimenko and R.W. Bilger, *Conditional moment closure for turbulent combustion*, Prog Energy Combust Sci **25** (1999), 595–687.

[13] K.K. Kuo (ed.), *Principles of combustion*, John Wiley and sons, 1986.

[14] S. K. Lele, *Compact finite difference schemes with spectral like resolution*, J. Comput. Phys. (1992), no. 103, 16–42.

[15] A. Linán and F. Williams, *Fundamentals aspects of combustion*, Oxford University Press, 1993.

[16] T. Mantel and R. Borghi, *A new model of premixed wrinkled flame propagation based on a scalar dissipation equation*, Combustion and Flame **96** (1994), 443–457.

[17] G.R Newman, B.E. Launder, and J.L. Lumley, *Modeling the behavior of homogeneous scalar turbulence*, Journal of fluids mechanics **111** (1982), 217–232.

[18] N. Peters, *Laminar flamelet concepts in turbulent combustion*, Proceedings of the 21rst Symposium (International) on combustion (Pittsburgh The combustion institute, ed.), 1986, pp. 1231–1250.

[19] C.D. Pierce and P. Moin, *A dynamic model for subgrid-scale variance and dissipation rate of a conserved scalar*, Phys. Fluids **10** (1998), no. 12, 3041–3044.

[20] T. Poinsot and D. Veynante, *Theoretical and numerical combustion*, Edwards, 2001.

[21] J. Reveillon, K.N.C. Bray, and L. Vervisch, *Dns study of spray vaporization and turbulent micro-mixing*, AIAA 98-1028 (36th Aerospace Sciences Meeting and Exhibit, January 12-15, Reno NV), January 1998.

[22] J. Reveillon and F.X. Demoulin, *Effects of the preferential segregation of droplets on evaporation and turbulent mixing*, Fluid Mech **583** (2007), 273–302.

[23] J. Réveillon and L. Vervisch, *Accounting for spray vaporization in non-premixed turbulent combustion modeling: A single droplet model (sdm)*, Combustion and Flame **1** (2000), no. 121, 75–90.

[24] J. Reveillon and L. Vervisch, *Analysis of weakly turbulent diluted-spray flames and spray combustion regimes*, J. Fluid Mech. (2005), no. 537, 317–347.

[25] L. Vervisch, B. Labeborre, and J. Reveillon, *Hydrogen-sulfur oxy-flame analysis and single-step flame tabulated chemistry*, Fuel (2004), no. 83, 605–614.

[26] L.P. Wang and M.R. Maxey, *Settling velocity and concentration distribution of heavy particles in homogeneous isotropic turbulence*, J. Fluid Mech. **256** (1993), 27–68.